On the torsion constant of multicell profiles and its maximization with respect to spar position

V.A. Lubarda *

Department of Mechanical and Aerospace Engineering, University of California, San Diego, La Jolla, CA 92093-0411, USA

ARTICLE INFO

ABSTRACT

A closed form expression for the torsion constant of thin-walled multicell profiles is derived based on a simple algorithm to generate the coefficient matrix of the system of linear algebraic equations for the shear flows. New explicit results are given for the three-cell profiles with either two or three internal walls, and for the two-cell profiles. They are applied to derive the optimal location of the internal walls which maximizes the torsion constant of triangular, rectangular, elliptical and deltoidal thin-walled profiles. The condition is also derived for the inner wall to carry a prescribed portion of the shear flow in a two-cell profile, with the application to thin-walled trapezoidal and rectangular profiles.

1. Introduction

The determination of the shear stresses and the angle of twist due to unconstrained torsion of a thin-walled prismatic rod with a multicell profile is a classical problem of structural mechanics [1–4]. Its solution is based on the well-known Bredt's formulas

$$2G\theta A_i = \oint_{C_i} \frac{f(s)}{\delta(s)}\, ds \quad (i = 1, 2, \ldots, n), \tag{1}$$

$$T = 2\sum_{i=1}^{n} f_i A_i, \tag{2}$$

in which θ is the angle of twist (per unit length) due to applied torque T, the shear modulus of the material is G, the shear flow along an external wall of the i-th cell is f_i, the area within the midline C_i of the i-th cell is A_i, and the wall thickness at an arbitrary position along the arc length s of the cell is $\delta(s)$. The total number of cells is n. The counterclockwise torque and twist are considered to be positive. The shear flow is defined in terms of the shear stress $\tau(s)$ by $f(s) = \tau(s)\delta(s)$, which is constant in between any two wall junctions. The sum of all shear flows toward any junction is equal to zero (by longitudinal equilibrium of the junction). Eqs. (1) and (2) constitute a set of $n+1$ coupled equations for n shear flows f_i and the angle of twist θ, which have

to be solved simultaneously. This is commonly done numerically, for each considered multicell profile. In doing so, the torsion constant is never calculated, although its numerical value can be extracted *a posteriori*, after the angle of twist is calculated, as $J = T/G\theta$.

The purpose of this paper is to derive directly an explicit expression for the torsion constant solely in terms of the geometrical properties of the multicell profile, which can then be used to calculate the angle of twist as $\theta = T/GJ$. Such procedure is a common practice in the study of torsion of prismatic bars with solid, thin-walled open, and single cell closed sections, for which the table listings of the corresponding expressions for J are routinely given. It is therefore desirable to do the same for the multicell sections. Having explicit expressions for the torsion constant of multicell profiles is important for the study of the torsion of prismatic bars with combined open-multicell closed sections (multicells with attached fins), for which the torsion constant of the entire profile is the sum of the multicell and fins contributions. Furthermore, having explicit expressions for the torsion constant enables an analytical study of the optimal arrangement of internal walls (spars) which maximizes the torsional stiffness of the structure. This is demonstrated in this paper by applying the derived expressions for the torsion constant of the two- and three-cell profiles to triangular, rectangular, elliptical and deltoidal thin-walled profiles. The conditions are also established for the inner wall to carry a prescribed portion of the shear flow, or no shear flow at all, with the application to two-cell trapezoidal and rectangular profiles.

* Tel.: +1 858 534 3169; fax: +1 858 534 5698.
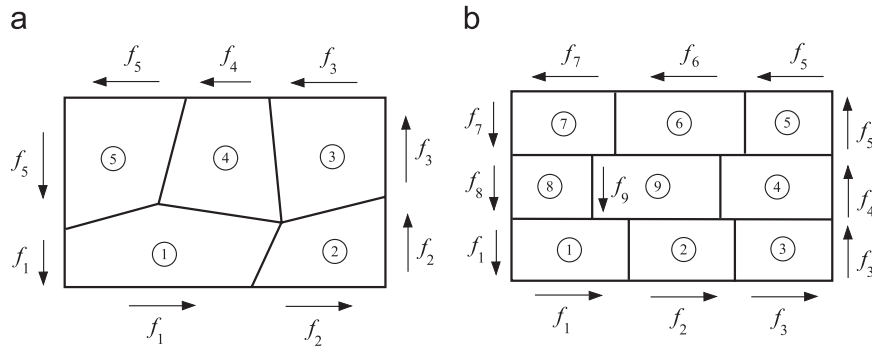*E-mail address:* vlubarda@ucsd.edu

Fig. 1. (a) A five-cell profile with indicated shear flows in external walls of the cells. (b) A nine-cell profile with indicated shear flows in external walls of the cells. The shear flow f_9 in the internal cell 9 is selected as shown in the figure.

2. Torsion constant of a multicell profile

The direct application of Eq. (1), in the form as it stands, while conceptually simple and straightforward [5–9], becomes awkward for profiles with many cells, because it requires a tedious integration of the shear stress $\tau(s) = f(s)/\delta(s)$ along all cells, with a careful identification of the shear flow and its direction in all internal walls of the cells. A simple algorithm to generate the system of equations for the shear flows f_i is based on the direct generation of the system matrix. This is accomplished by observing that the contour integrals (1) can be expressed as

$$\oint_{C_i} \frac{f(s)}{\delta(s)}\, ds = I_{ii}f_i + \sum_{j\in\mathcal{N}_i} I_{ij}f_j, \tag{3}$$

where

$$I_{ii} = \oint_{C_i} \frac{ds}{\delta(s)}, \quad I_{ij} = -\int_{C_{i,j}} \frac{ds}{\delta(s)} \tag{4}$$

are the nondimensional parameters referred to as the flexibility coefficients [4]. In (3) and (4), $C_{i,j}$ denotes the internal wall segment between the i-th and j-th cell, and $\mathcal{N}_i$ is the union of all neighboring cells sharing the wall with the i-th cell. For example, for the profile in Fig. 1a, $\mathcal{N}_4 = \{1,3,5\}$, while for the profile in Fig. 1b, $\mathcal{N}_9 = \{1,2,4,6,7\}$.[1] Therefore, the system of linear algebraic equations for the n shear flows is

$$\sum_{j=i}^{j\in\mathcal{N}_i} I_{ij}f_j = 2G\theta A_i \quad (i = 1,2,\ldots,n). \tag{5}$$

The solution of this system is

$$f_i = 2G\theta \frac{D_i}{D} \quad (i = 1,2,\ldots,n), \tag{6}$$

where $D = \det(I_{ij})$ is the determinant, and $2G\theta D_i$ is the i-th cofactor of the system matrix (I_{ij}), corresponding to f_i. When (6) is substituted into (2), the applied torque becomes

$$T = \frac{4G\theta}{D} \sum_{i=1}^{n} A_i D_i. \tag{7}$$

This establishes an expression for the torsion constant, defined as $J = T/G\theta$, explicitly in terms of the geometrical properties of the profile,

$$J = \frac{4}{D} \sum_{i=1}^{n} A_i D_i. \tag{8}$$

---

[1] If a cell is entirely an inside cell, with no external walls, such as the cell 9 in Fig. 1b, the shear flow in any of its walls can be chosen as f_9. If the shear flow in the wall between the cell p and q is chosen as f_p, then $I_{pq} = 0$. Thus, $I_{89} = 0$ for the profile with f_9 as chosen in Fig. 1b.

The shear flows can be expressed, from (6) to (8), as

$$f_i = \frac{D_i}{\sum_1^n A_i D_i} \frac{T}{2} \quad (i = 1,2,\ldots,n). \tag{9}$$

Evidently, $f_i = f_j$ if and only if $D_i = D_j$. Having determined f_i, the shear flows f_{ij} in the inner walls follow from the equations expressing the longitudinal equilibrium of each junction (Kirchhoff law for the shear flows at the junction).

2.1. The structure of the system matrix

The structure of the system matrices corresponding to five- and nine-cell profiles shown in Fig. 1 is

$$(I_{ij}) = \begin{pmatrix} I_{11} & I_{12} & I_{13} & 0 & 0 \\ I_{21} & I_{22} & I_{23} & I_{24} & 0 \\ I_{31} & I_{32} & I_{33} & 0 & I_{35} \\ 0 & I_{42} & 0 & I_{44} & I_{45} \\ 0 & 0 & I_{53} & I_{54} & I_{55} \end{pmatrix} \tag{10}$$

and

$$(I_{ij}) = \begin{pmatrix} I_{11} & I_{12} & 0 & 0 & 0 & 0 & 0 & I_{18} & I_{19} \\ I_{21} & I_{22} & I_{23} & I_{24} & 0 & 0 & 0 & 0 & I_{29} \\ 0 & I_{32} & I_{33} & I_{34} & 0 & 0 & 0 & 0 & 0 \\ 0 & I_{42} & I_{43} & I_{44} & I_{45} & I_{46} & 0 & 0 & I_{49} \\ 0 & 0 & 0 & I_{54} & I_{55} & I_{56} & 0 & 0 & 0 \\ 0 & 0 & 0 & I_{64} & I_{65} & I_{66} & I_{67} & 0 & I_{69} \\ 0 & 0 & 0 & 0 & 0 & I_{76} & I_{77} & I_{78} & I_{79} \\ I_{81} & 0 & 0 & 0 & 0 & 0 & I_{87} & I_{88} & 0 \\ I_{91} & I_{92} & 0 & I_{94} & 0 & I_{96} & I_{97} & 0 & I_{99} \end{pmatrix}. \tag{11}$$

If the profile consists of cells arranged one-by-one (next to each other), the coefficient matrix is trigonal, because each cell (compartment) is surrounded by two neighboring cells, except the first and the last cell, which have only one neighboring cell [2–4].

3. Torsion constant of a three-cell profile

In the case of a three-cell profile (Fig. 2a), the elements of the system matrix,

$$(I_{ij}) = \begin{pmatrix} I_{11} & I_{12} & I_{13} \\ I_{21} & I_{22} & I_{23} \\ I_{31} & I_{32} & I_{33} \end{pmatrix}, \tag{12}$$
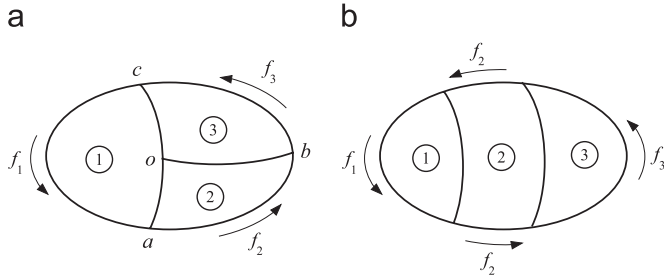
a b

Fig. 2. (a) A three-cell profile with indicated shear flows along the external walls of the profile. The internal walls are *oa*, *ob*, and *oc*. (b) A three-cell profile with the cells arranged next to each other.

a b

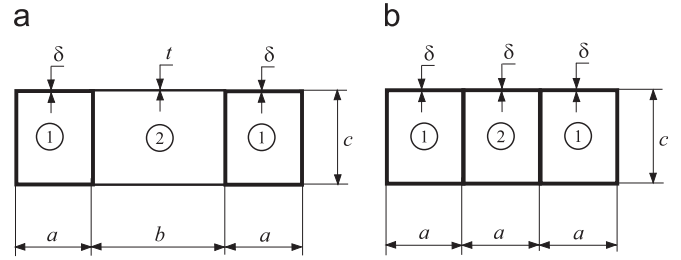**Fig. 3.** (a) A three-cell rectangular profile with identical outside cells. (b) A three-cell rectangular profile with identical cells.

are the nondimensional parameters

$$I_{ii} = \oint_{C_i} \frac{ds}{\delta(s)} \quad (i = 1, 2, 3),$$

$$I_{12} = -\int_0^a \frac{ds}{\delta(s)}, \quad I_{23} = -\int_0^b \frac{ds}{\delta(s)}, \quad I_{31} = -\int_0^c \frac{ds}{\delta(s)}. \tag{13}$$

The determinant of the matrix is

$$D = I_{11}I_{22}I_{33} - I_{11}I_{23}^2 - I_{22}I_{31}^2 - I_{33}I_{12}^2 + 2I_{12}I_{23}I_{31}. \tag{14}$$

The cofactor parameters are

$$D_i = A_i(I_{jj}I_{kk} - I_{jk}^2) + A_j(I_{ki}I_{kj} - I_{kk}I_{ij}) + A_k(I_{ij}I_{jk} - I_{jj}I_{ki}), \tag{15}$$

where (i, j, k) is a set of integers $(1, 2, 3)$, or its other two even permutations, $(2, 3, 1)$ and $(3, 1, 2)$. It readily follows that

$$\sum_{i=1}^3 A_i D_i = A_1^2(I_{22}I_{33} - I_{23}^2) + A_2^2(I_{33}I_{11} - I_{31}^2) + A_3^2(I_{11}I_{22} - I_{12}^2)$$
$$+ 2A_1A_2(I_{31}I_{23} - I_{33}I_{12}) + 2A_2A_3(I_{12}I_{31} - I_{11}I_{23})$$
$$+ 2A_3A_1(I_{12}I_{23} - I_{22}I_{31}).$$

If the cells 1 and 3 have no common wall (Fig. 2b), the previous expressions simplify, because $I_{13} = I_{31} = 0$. For example, the determinant (14) reduces to $D = I_{11}I_{22}I_{33} - I_{11}I_{23}^2 - I_{33}I_{12}^2$. In this case, if the internal walls are such that $I_{12} = I_{23}$ (e.g., same height and thickness), the torsion constant becomes

$$J = 4\frac{A_1^2 I_2 I_3 + A_2^2 I_3 I_1 + A_3^2 I_1 I_2 - (A_1 - A_3)^2 I_0^2 - 2(A_1 I_3 + A_3 I_1)A_2 I_0}{I_1 I_2 I_3 - (I_1 + I_3) I_0^2}. \tag{16}$$

For brevity, we used in this expression the notation $I_{12} = I_{23} = I_0$ and $I_{ii} = I_i$. Furthermore, if the two outside cells are characterized by $A_1 = A_3$ and $I_{11} = I_{33}$, the torsion constant (16) reduces to

$$J = 4\frac{2A_1^2 I_{22} + A_2^2 I_{11} - 4A_1 A_2 I_{12}}{I_{11}I_{22} - 2I_{12}^2}. \tag{17}$$

This expression applies, for example, to a three-cell profile shown in Fig. 3a. It also applies to a wide range of structurally important three-cell profiles, such as thin-walled elliptical and deltoidal profiles. The expression (17), previously not reported in the literature, greatly facilitates some aspects of the structural optimization analysis, such as the determination of the location of the internal spars which maximizes the torsion constant of a three-cell profiles. This is discussed in Sections 3.2 and 3.3 of this paper. The shear flows corresponding to (17) are

$$f_1 = \frac{A_1 I_{22} - A_2 I_{12}}{2A_1^2 I_{22} + A_2^2 I_{11} - 4A_1 A_2 I_{12}} \frac{T}{2},$$

$$f_2 = \frac{A_2 I_{11} - 2A_1 I_{12}}{2A_1^2 I_{22} + A_2^2 I_{11} - 4A_1 A_2 I_{12}} \frac{T}{2}. \tag{18}$$

If $A_1 = A_2 = A_3$, but $t \neq \delta$, (17) simplifies to

$$J = 4A_1^2 \frac{I_{11} + 2I_{22} - 4I_{12}}{I_{11}I_{22} - 2I_{12}^2}. \tag{19}$$

Finally, for a profile with uniform thickness and equal cells ($t = \delta$, $I_{11} = I_{22}$), shown in Fig. 3b, the torsion constant is

$$J = 4A_1^2 \frac{3I_{11} - 4I_{12}}{I_{11}^2 - 2I_{12}^2}. \tag{20}$$

Since $A_1 = ac$, $I_{11} = 2(a + c)/\delta$, and $I_{12} = -c/\delta$, the above becomes

$$J = 4a^2 c^2 \frac{(3a + 5c)\delta}{2a^2 + 4ac + c^2}. \tag{21}$$

3.1. Thin-walled rectangular profile with two spars

For the symmetric three-cell profile shown in Fig. 4a, with the thickness δ of external walls and the thickness t of internal (spar) walls, we have $A_1 = ac$, $A_2 = bc$, and

$$I_{11} = \frac{2a + c}{\delta} + \frac{c}{t}, \quad I_{22} = \frac{2(h - 2a)}{\delta} + \frac{2c}{t}, \quad I_{12} = -\frac{c}{t}.$$

The substitution into (17) yields the following expression for the torsion constant:

$$J = 2h^2 c\delta \frac{1 + (1 - 2a/h)[1 - 2(a/h) + 2\alpha(a/h)]t/\delta}{1 + \alpha + \alpha(1 + 2\alpha a/h)(1 - 2a/h)t/\delta}, \tag{22}$$

where $\alpha = h/c$. The plots of J vs. a/h, for several specified thickness ratios t/δ (0.5, 1, 2), are shown in Fig. 5a. For a given h, the length a is in the range $(\delta + t)/2 \leqslant a \leqslant h - t$, so that the ratio a/h is bounded by

$$\frac{1}{2}\beta\left(1 + \frac{t}{\delta}\right) \leqslant \frac{a}{h} \leqslant \frac{1}{2}\left(1 - \beta\frac{t}{\delta}\right), \tag{23}$$

where $\beta = \delta/h$. The plots in Fig. 5a correspond to $\alpha = 3$ and $\beta = \frac{1}{30}$, indicating that the torsion constant J is a decreasing function of the ratio a/h. Thus, placing the spars toward the middle of the cross section decreases the torsion constant. Physically, this is because the nearby spars around the middle of the cross section (Fig. 4b) carry a small portion of the applied torque (due to their small moment arm length). The decrease of J with the increase of a/h is more pronounced for the thicker spars.

Fig. 5b shows the variation of J with t/δ in the case $\alpha = 3$ and $\beta = \frac{1}{30}$, and for the three selected values of the ratio $a/h = 0.2, 0.3, 0.4$. The plots quantify the expected increase of the torsion constant with the increase of the spar thickness. In the case $a/h = 0.2$, doubling the spar thickness from $t = \delta$ to 2δ increases the torsion constant from $J = 0.2613$ to 0.2651 (scaled by $2h^2 c\delta$). The increase is less pronounced for higher values of the ratio a/h, and for $a/h = 0.4$, the increase is from $J = 0.2517$ to $0.2525 \times (2h^2 c\delta)$.
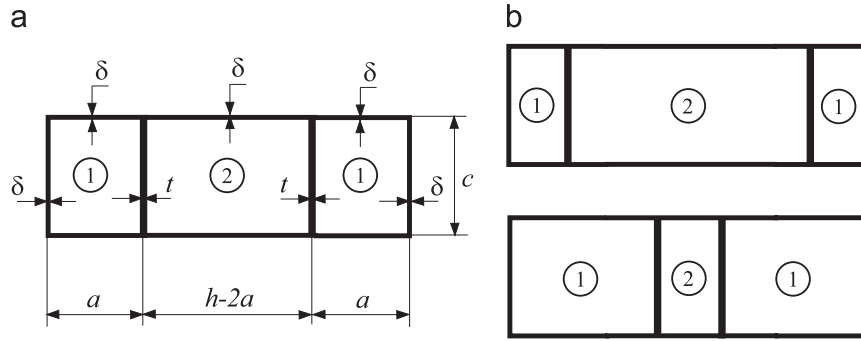
Fig. 4. (a) A three-cell rectangular profile with identical outside cells. The thickness of external walls is δ, and the thickness of internal walls is t. (b) The three-cell rectangular profiles with remote and nearby internal walls. The torsion constant is smaller in the case of nearby walls.
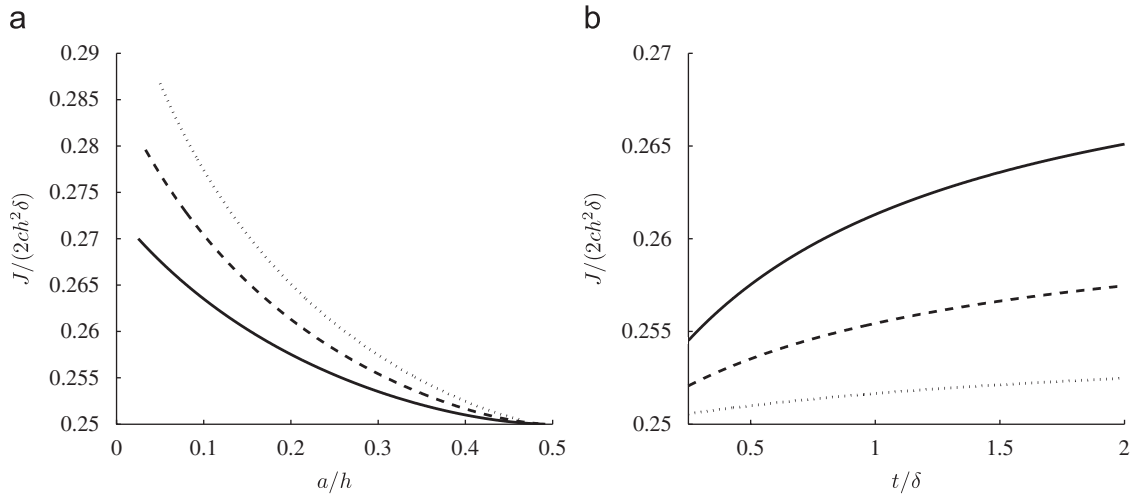

Fig. 5. (a) The variation of the torsion constant J with the ratio a/h, for the three-cell profile from Fig. 4a. The solid curve corresponds to the thickness ratio $t/\delta = \frac{1}{2}$, the dashed curve is for $t/\delta = 1$, and the dotted curve is for $t/\delta = 2$. (b) The variation of the torsion constant J with the thickness ratio t/δ. The solid curve corresponds to $a/h = 0.2$ (remote spars), the dashed curve is for $a/h = 0.3$, and the dotted curve for is $a/h = 0.4$ (nearby spars).

3.2. Thin-walled circular and elliptical profiles with two spars

Fig. 6a shows a thin-walled circular profile of mid-radius a and the wall thickness δ. Two vertical spars of thickness t are positioned at the distance x from the center, such that $\sin\varphi = x/a$. It is readily found that

$$A_1 = a^2\left(\frac{\pi}{2} - \varphi - \sin\varphi\cos\varphi\right), \quad A_2 = 2a^2(\varphi + \sin\varphi\cos\varphi),$$

$$I_{11} = 2\frac{a}{t}\left[\cos\varphi + \left(\frac{\pi}{2} - \varphi\right)\frac{t}{\delta}\right], \quad I_{22} = 4\frac{a}{t}\left(\cos\varphi + \varphi\frac{t}{\delta}\right),$$

$$I_{12} = -2\frac{a}{t}\cos\varphi.$$

The substitution into (17) yields the following expression for the torsion constant:

$$J = 2\pi a^3\delta\,\frac{\frac{\pi}{2}\cos\varphi + \left(\frac{\pi}{2}\varphi - \varphi^2 + \sin^2\varphi\cos^2\varphi\right)\frac{t}{\delta}}{\frac{\pi}{2}\cos\varphi + \varphi\left(\frac{\pi}{2} - \varphi\right)\frac{t}{\delta}}. \tag{24}$$

The corresponding variation of J with x/a is shown in Fig. 7a. For $t/\delta = 0.5$, the cross section has the greatest torsion constant if the spars are located at $x/a = 0.7963$, and $J_{\max} = 1.0929 \times (2\pi a^3\delta)$. For $t/\delta = 1$, the optimal distance is $x/a = 0.7781$, with the corresponding $J_{\max} = 1.15 \times (2\pi a^3\delta)$, while for $t/\delta = 2$, the distance is $x/a = 0.7651$ and $J_{\max} = 1.2176 \times (2\pi a^3\delta)$. If the spars are nearby each other, in the middle of the profile, their net contribution to the torsion constant is nearly zero, and
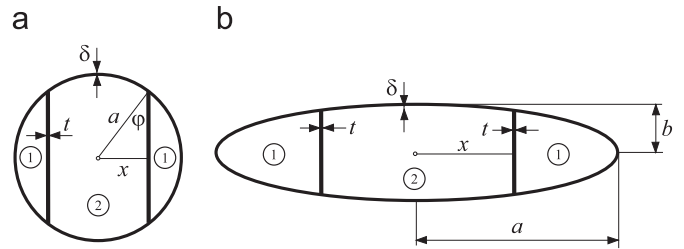

Fig. 6. (a) A thin-walled circular profile with two spars located at the distance x from the center. (b) A thin-walled elliptical profile with two spars at the distance x from the center.

$J \to 2\pi a^3\delta$, which corresponds to a circular tube of radius a and thickness δ.

Similar analysis can be performed for a thin-walled elliptical profile with the semi-axes a and b and the wall thickness δ, which is stiffened by two spars of thickness t at the distance x from the center (Fig. 6b). Introducing the angle $\varphi = \sin^{-1}(x/a)$, there follows:

$$A_1 = ab\left[\frac{\pi}{2} - \varphi - \frac{1}{2}\sin(2\varphi)\right], \quad A_2 = ab[2\varphi + \sin(2\varphi)],$$

$$I_{11} = 2\frac{a}{\delta}[E(\pi/2, e) - E(\varphi, e)] + 2\frac{b}{t}\cos\varphi$$

$$I_{22} = 4\frac{a}{\delta}E(\varphi, e) + 4\frac{b}{t}\cos\varphi$$

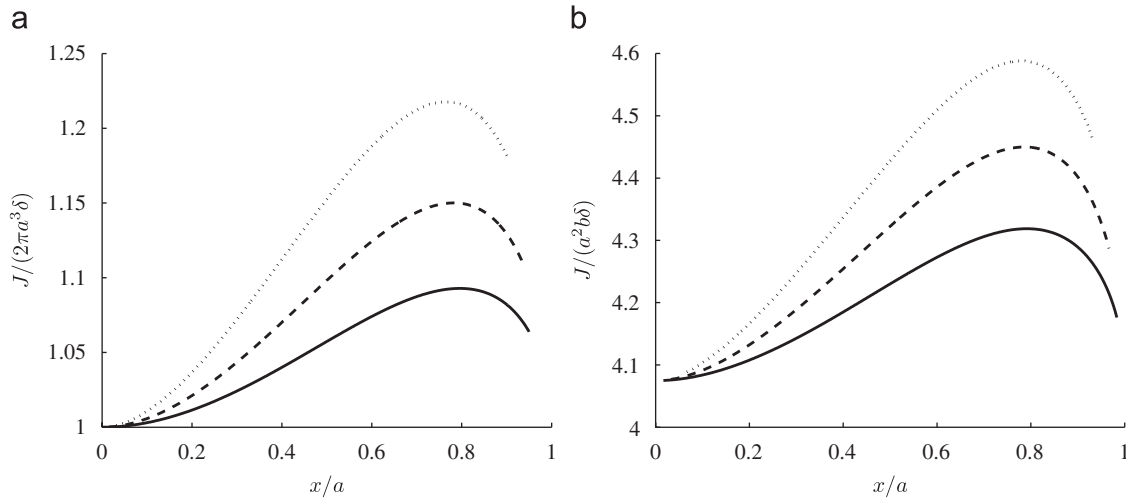$$I_{12} = -2\frac{b}{t}\cos\varphi, \quad e = (1 - b^2/a^2)^{1/2}, \tag{25}$$

a

b

Fig. 7. (a) The variation of the torsion constant J with x/a for the circular profile with $\delta = a/15$. The solid curve corresponds to the thickness ratio $t/\delta = \frac{1}{2}$, the dashed curve is for $t/\delta = 1$, and the dotted curve is for $t/\delta = 2$. (b) The same for the elliptical profile from Fig. 6b, with $b = a/3$.
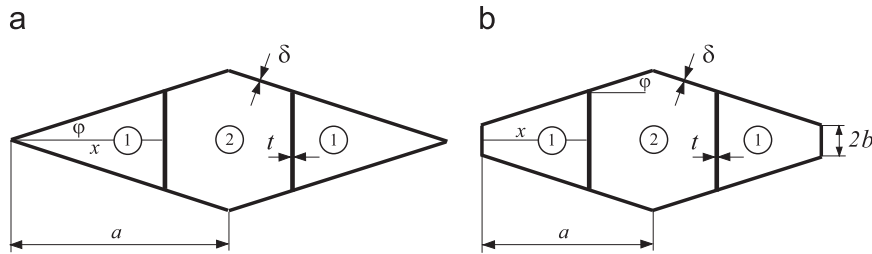
a

b

Fig. 8. (a) A thin-walled deltoidal profile with two spars at the distance x from the ends. (b) A truncated thin-walled deltoidal profile.

where e is the eccentricity of the ellipse, and

$$E(\varphi, e) = \int_0^{\varphi} (1 - e^2 \sin^2 \varphi)^{1/2} \, d\varphi \qquad (26)$$

is the elliptic integral of the second kind. The substitution of (25) into (17) yields an involved expression for the torsion constant, which can be easily evaluated by using the Mathematica or Mathlab software packages, for any eccentricity of the ellipse and any thickness ratio t/δ. Fig. 7b shows the variation of the torsion constant with the spar distance x in the case $t/\delta = (0.5, 1, 2)$, the semi-axes ratio $a/b = 3$ ($e^2 = \frac{8}{9}$), and the thickness $\delta = a/15$. The maximum torsion constant in these three cases is $J_{\max} = (3.0962, 3.1642, 3.2303)a^2 b\delta$, with the corresponding spars located at $x/a = (0.7737, 0.7738, 0.7733)$. The optimal location of spars for maximum torsion constant depends on the eccentricity of the ellipse. If $e^2 = \frac{3}{4}$ (i.e., $a/b = 2$), one finds, in the same cases of the thickness ratios t/δ and δ/a, that $x/a = (0.7916, 0.7858, 0.7805)$. The corresponding torsion constants are $J_{\max} = (4.3187, 4.4499, 4.5881)a^2 b\delta$. Similar analysis can be performed in the case of a semi-elliptical thin-walled profile shown in Fig. 10a, but details are omitted for brevity.

3.3. Thin-walled deltoidal profile with two spars

A thin-walled deltoidal profile shown in Fig. 8a has a half-length a, the inclination angle φ, and the thickness of the outer walls δ. The two symmetrically positioned spars at the distance x from the ends have the thickness t. It readily follows that

$$A_1 = x^2 \tan \varphi, \quad A_2 = 2a^2 \tan \varphi \left(1 - \frac{x^2}{a^2}\right), \quad I_{12} = -2\frac{x}{t}\tan \varphi,$$

$$I_{11} = 2\frac{x}{t}\frac{1}{\cos \varphi}\left(\sin \varphi + \frac{t}{\delta}\right), \quad I_{22} = 4\frac{a}{t}\frac{1}{\cos \varphi}\left[\sin \varphi \frac{x}{a} + \left(1 - \frac{x}{a}\right)\frac{t}{\delta}\right].$$

The substitution into (17) yields the following expression for the torsion constant:

$$J = 4a^3 \delta \frac{\sin^2 \varphi}{\cos \varphi} \frac{\sin \varphi + \left(1 - 2\dfrac{x^2}{a^2} + \dfrac{x^3}{a^3}\right)\dfrac{t}{\delta}}{\sin \varphi + \left(1 - \dfrac{x}{a}\right)\dfrac{t}{\delta}}. \qquad (27)$$

The plots shown in Fig. 9a correspond to $\varphi = 15°$ and $\delta = a/15$. For $t/\delta = 0.5$, the cross section has the maximum torsion constant if the spars are located at $x/a = 0.4056$, and $J_{\max} = 0.3132a^3\delta$. For $t/\delta = 1$, the optimal location is $x/a = 0.4325$, with $J_{\max} = 0.324a^3\delta$, while for $t/\delta = 2$ it is found that $x/a = 0.4558$, and $J_{\max} = 0.3328a^3\delta$.

Similar analysis can be performed for a truncated deltoidal profile shown in Fig. 8b, for which

$$A_1 = (2b + x \tan \varphi)x, \quad A_2 = 2[2b + (a + x) \tan \varphi](a - x),$$

$$I_{11} = \frac{2x}{\delta \cos \varphi} + \frac{2b}{\delta} + \frac{2(b + x \tan \varphi)}{t},$$

$$I_{22} = \frac{4(a - x)}{\delta \cos \varphi} + \frac{4(b + x \tan \varphi)}{t},$$

$$I_{12} = -\frac{2(b + x \tan \varphi)}{t}. \qquad (28)$$

The corresponding plots of J vs. x/a, calculated from (17) in the case $a/b = 8$, are shown in Fig. 9b. For $t/\delta = 0.5$, the maximum torsion constant $J_{\max} = 0.9781a^3\delta$ is attained for $x/a = 0.2889$. For $t/\delta = 1$, the optimal location is $x/a = 0.2962$ with $J_{\max} = 1.001a^3\delta$, while for $t/\delta = 2$, $x/a = 0.3058$ and $J_{\max} = 1.0219a^3\delta$. Similar analysis can be performed in the case of a triangular thin-walled profile shown in Fig. 10b.
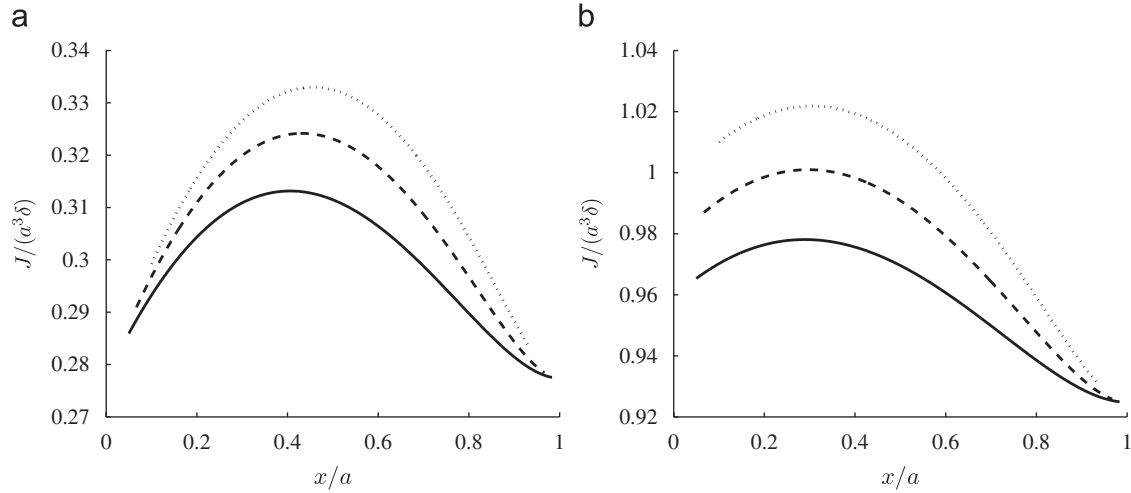
Fig. 9. (a) The variation of the torsion constant J with x/a for the deltoidal profile with $\varphi = 15°$ and $\delta = a/15$. The solid curve corresponds to the thickness ratio $t/\delta = \frac{1}{2}$, the dashed curve is for $t/\delta = 1$, and the dotted curve is for $t/\delta = 2$. (b) The same for the truncated deltoidal profile from Fig. 8b, with $b = a/8$.
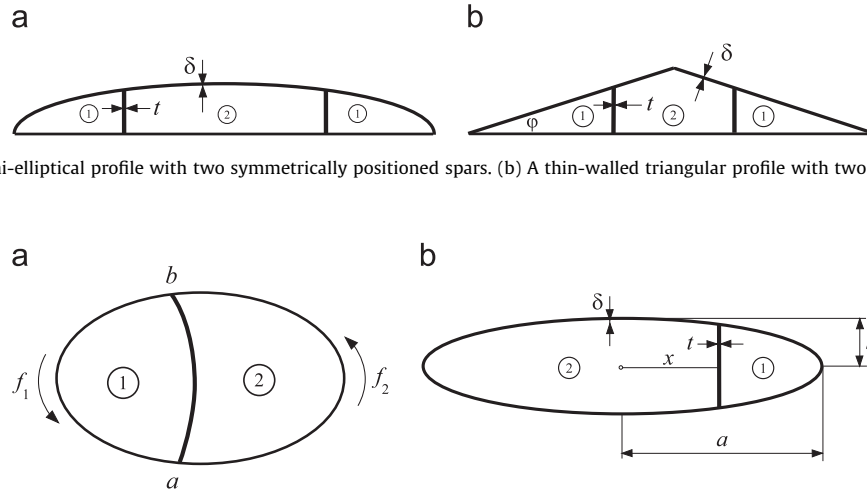

Fig. 10. (a) A thin-walled semi-elliptical profile with two symmetrically positioned spars. (b) A thin-walled triangular profile with two symmetrically positioned spars.
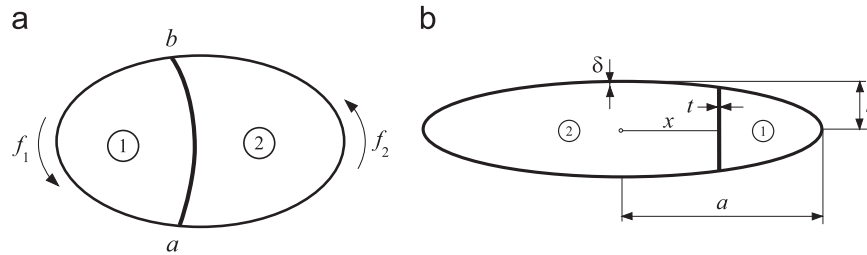

Fig. 11. (a) A two-cell profile with indicated shear flows f_1 and f_2 in the external walls of the profile. The internal wall is ab. (b) A two-cell elliptical profile with a spar at the distance x from the center of the ellipse.

4. Torsion constant of a two-cell profile

In the case of a two-cell profile (Fig. 11a), the elements of the system matrix,

$$(I_{ij}) = \begin{pmatrix} I_{11} & I_{12} \\ I_{21} & I_{22} \end{pmatrix}, \tag{29}$$

are

$$I_{11} = \oint_{C_1} \frac{ds}{\delta(s)}, \quad I_{22} = \oint_{C_2} \frac{ds}{\delta(s)}, \quad I_{12} = -\int_a^b \frac{ds}{\delta(s)}. \tag{30}$$

The determinant of the matrix is $D = I_{11}I_{22} - I_{12}^2$, and

$$D_1 = A_1 I_{22} - A_2 I_{12}, \quad D_2 = A_2 I_{11} - A_1 I_{21}. \tag{31}$$

The torsion constant is readily found to be

$$J = 4 \frac{A_1^2 I_{22} + A_2^2 I_{11} - 2A_1 A_2 I_{12}}{I_{11}I_{22} - I_{12}^2}, \tag{32}$$

explicitly expressed in terms of the geometric properties alone. Surprisingly, this simple expression for the torsion constant of a

two-cell profile does not appear in the literature on thin-walled structures. The corresponding shear flows are

$$f_1 = \frac{A_1 I_{22} - A_2 I_{12}}{A_1^2 I_{22} + A_2^2 I_{11} - 2A_1 A_2 I_{12}} \frac{T}{2},$$

$$f_2 = \frac{A_2 I_{11} - A_1 I_{21}}{A_1^2 I_{22} + A_2^2 I_{11} - 2A_1 A_2 I_{12}} \frac{T}{2}, \tag{33}$$

in agreement with the expressions (17.51) of Ref. [3]. Observe also the duality between (32) and (33) and the corresponding expressions (17) and (18) for the symmetric three-cell profiles.

The inner wall carries no shear stress if and only if $f_1 = f_2$, i.e.,

$$A_1(I_{21} + I_{22}) = A_2(I_{11} + I_{12}). \tag{34}$$

If the ratio of the shear flows in external walls is to be equal to k ($f_2 = kf_1$), the shear flow in the inner wall being $f_{12} = (1 - k)f_1$, the expression (34) generalizes to

$$A_1(I_{21} + kI_{22}) = A_2(I_{11} + kI_{12}). \tag{35}$$

This condition can be useful in the design analysis. For example, it can be achieved by the adjustment of the wall thicknesses of the cells, as discussed in Section 4.2.
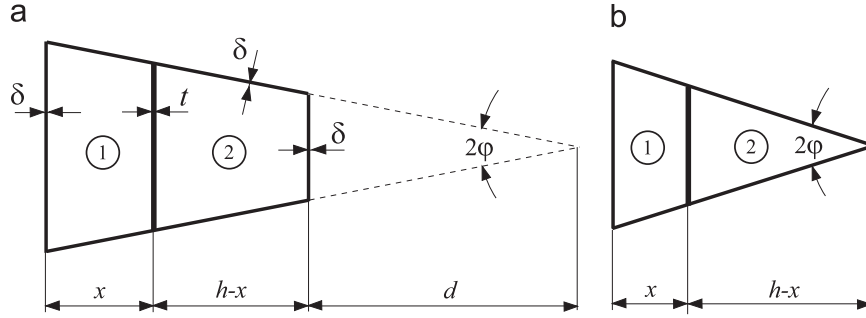
Fig. 12. (a) A two-cell trapezoidal profile of height h, the external wall thickness δ, and the spar thickness t. The parameters d and φ specify the steepness of the trapezoid. (b) A triangular two-cell profile deduced from the trapezoidal profile in the limit $d \to 0$.

In the case (34) holds, (32) reduces to a single-cell Bredt's formula

$$J = \frac{4A^2}{I}, \quad I = I_{11} + I_{22} + 2I_{12} = \int_C \frac{\mathrm{d}s}{\delta(s)}, \tag{36}$$

where $A = A_1 + A_2$ is the area within the external contour C of the profile (without the internal wall), and I is the corresponding integral of the reciprocal of the wall thickness.[2] In particular, (34) holds if $A_1 = A_2$ and $I_{11} = I_{22}$. Two illustrative examples are discussed in the following subsections.

4.1. Two-cell trapezoidal profile

Fig. 12a shows a two-cell trapezoidal profile of height h, thickness δ, and the steepness specified by the geometric parameters d and φ. The spar of thickness t is located at the distance x from the left end. From (30) it readily follows that

$$I_{11} = \frac{2h}{t \cos \varphi}\left[(1+\alpha)\left(1+\frac{t}{\delta}\right)\sin \varphi + \left(\frac{t}{\delta} - \sin \varphi\right)\frac{x}{h}\right],$$

$$I_{22} = \frac{2h}{t \cos \varphi}\left[\left(\frac{t}{\delta} + \sin \varphi\right)\left(1 - \frac{x}{h}\right) + \left(1+\frac{t}{\delta}\right)\alpha \sin \varphi\right],$$

$$I_{12} = -\frac{2h}{t \cos \varphi}\left(1 + \alpha - \frac{x}{h}\right)\sin \varphi, \tag{37}$$

where $\alpha = d/h \geqslant 0$. The areas within the two cells are

$$A_1 = \frac{x}{h}\left[2(1+\alpha) - \frac{x}{h}\right]h^2 \tan \varphi, \quad A_2 = \left(1 - \frac{x}{h}\right)\left(1 + 2\alpha - \frac{x}{h}\right)h^2 \tan \varphi. \tag{38}$$

The sufficient conditions for the vanishing of the shear flow in the internal wall ($f_{1-2} = 0$, i.e., $f_1 = f_2$) are $A_1 = A_2$ and $I_{11} = I_{22}$. They give

$$\frac{x}{h} = 1 + \alpha - \left(\frac{1}{2} + \alpha + \alpha^2\right)^{1/2}, \quad \sin \varphi = 1 - 2\frac{x}{h}. \tag{39}$$

Since $\sin \varphi \leqslant 1$, the location of the shear-free spar in (39) satisfies the inequality $x/h \leqslant \frac{1}{2}$.

We can also determine at what distance x the spar should be located to maximize the torsion constant of the trapezoidal two-cell profile. The substitution of (37) and (38) into (32) yields an expression for the torsion constant, whose variation with x/h is shown in Fig. 13a in the case of the thickness ratio $t/\delta = (0.5, 1, 2)$, the angle $\varphi = 15°$, $\delta/h = \frac{1}{15}$, and $\alpha = 1$. As seen from this figure, the torsion constant is the greatest when the spar is located close to the larger base of the trapezoid. The minimum value of the torsion constant $J_{\min} \approx 0.3513 \times (2h^3\delta)$ is attained at $x/h \approx 0.4766$, regardless of the thickness ratio t/δ, because this

corresponds to the shear-free spar location. The shape of the curve $J = J(x)$ sensitively depends on the steepness of the trapezoid. For example if $\alpha = c/h = 0.25$ and $\varphi = 15°$, the curve $J = J(x)$ has both its minimum and maximum inside of the span h. For example, if $t = \delta$, the minimum torsion constant is $J_{\min} = 0.1124 \times (2h^3\delta)$ at $x/h = 0.3171$, while the maximum torsion constant is $J_{\max} = 0.1169 \times (2h^3\delta)$ at $x/h = 0.8094$.

Fig. 13b shows the variation of J with x/h, for various thickness ratios t/δ, in the case of a two-cell triangular profile from Fig. 12b, which is obtained from the general expression for the trapezoidal profile by setting $d = 0$ (i.e., $\alpha = 0$). The explicit expression for J is

$$J = 2h^3\delta \tan \varphi \sin \varphi \frac{\sin \varphi + [1 - 2\eta^2 + (1 + \sin \varphi)\eta^3](t/\delta)}{\sin \varphi(1 + \sin \varphi) + (1 + \sin \varphi - \eta)(t/\delta)}, \tag{40}$$

where $\eta = 1 - x/h$. The parameters used in calculations for the plots shown in Fig. 13b were $\varphi = 15°$ and $\delta/h = \frac{1}{15}$. The plots reveal that the considered triangular profile attains the maximum torsion constant if its spar is located at the distance $x/h = (0.7052, 0.6967, 0.6904)$, corresponding to the thickness ratio $t/\delta = (0.5, 1, 2)$, demonstrating a mild dependence of the optimal location x on the spar thickness. The minimum torsion constant $J_{\min} \approx 0.0551 \times (2h^3\delta)$ corresponds to a shear-free spar, which is located at $x/h \approx 0.205$, regardless of the thickness ratio t/δ.

4.2. Two-cell rectangular profile

In this subsection we first apply the condition (35) to determine the thickness ratio t/δ for the two-cell rectangular profile shown in Fig. 14a, for which the ratio of the shear flows in the external walls of the profile is $f_2/f_1 = k$. The areas within the cells are $A_1 = a^2$ and $A_2 = ab$, while

$$I_{11} = \frac{4a}{\delta}, \quad I_{22} = \frac{a}{\delta} + \frac{a + 2b}{t}, \quad I_{12} = -\frac{a}{\delta}, \tag{41}$$

so that, from (32), the corresponding torsion constant is

$$J = 4a^3\delta \frac{1 + 2\dfrac{b}{a} + \left(1 + 2\dfrac{b}{a} + 4\dfrac{b^2}{a^2}\right)\dfrac{t}{\delta}}{4\left(1 + 2\dfrac{b}{a}\right) + 3\dfrac{t}{\delta}}. \tag{42}$$

The substitution of (41) into (35) gives

$$A_1(I_{21} + kI_{22}) = A_2(I_{11} + kI_{12}) \quad \Rightarrow \quad \frac{t}{\delta} = \frac{k(a + 2b)}{(1-k)a + (4-k)b}. \tag{43}$$

With this wall thickness ratio, (42) reduces to a remarkably simple expression

---

[2] If (34) holds, then $A_1 = A(I_{11} + I_{12})/I$, $A_2 = A(I_{21} + I_{22})/I$, and the substitution into (32), after a somewhat lengthy derivation, yields (36).
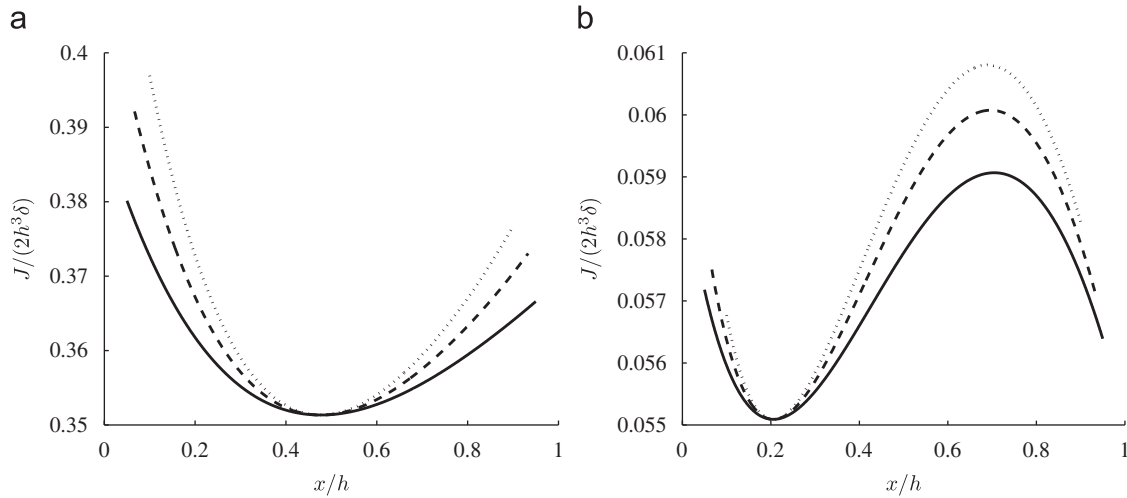
$$J = 4a^2\delta \frac{a + kb}{4 - k}. \tag{44}$$

a

b

Fig. 13. (a) The variation of the torsion constant J with x/h for the trapezoidal profile from Fig. 12a, with $c = h$, $\varphi = 15°$, and $\delta = h/15$. The solid curve corresponds to the thickness ratio $t/\delta = \frac{1}{2}$, the dashed curve is for $t/\delta = 1$, and the dotted curve is for $t/\delta = 2$. (b) The same for the triangular profile ($d = 0$) from Fig. 12b.
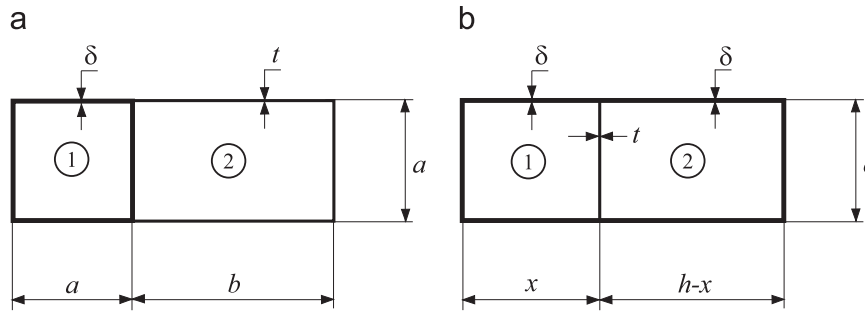
a

b

Fig. 14. (a) A two-cell rectangular profile with the cell sides $a \times a$ and $b \times a$, and the indicated thicknesses δ and t. (b) A two-cell rectangular profile of dimensions $h \times c$ and uniform external-wall thickness δ, stiffened by a spar of thickness t at the distance x from the left end.

If the inner wall is to carry no shear stress at all ($k = 1$), the thickness ratio must be $t/\delta = (a + 2b)/(3b)$, while the torsion constant becomes $J = 4a^2\delta(a + b)/3$. In this case, $t \leqslant \delta$ if $b \geqslant a$, and vice versa. If $a = b$, then $t = \delta$, which is also obvious by the symmetry consideration, and $J = 8a^3\delta/3$.

Next, it is of interest to determine the location x of the vertical spar of thickness t in a rectangular profile of dimensions $h \times c$ and the external wall thickness δ (Fig. 14b) for which the corresponding torsion constant attains its maximum value. The areas within the two cells are $A_1 = xc$ and $A_2 = (h - x)c$, while

$$I_{11} = \frac{2x}{\delta} + \frac{c}{\delta} + \frac{c}{t}, \quad I_{22} = \frac{2(h - x)}{\delta} + \frac{c}{\delta} + \frac{c}{t}, \quad I_{12} = -\frac{c}{t}. \quad (45)$$

The substitution into (32) gives

$$J = 4ch^2\delta \frac{1 + \left[1 - 2(1 - \alpha)\frac{x}{h}\left(1 - \frac{x}{h}\right)\right]\frac{t}{\delta}}{2(1 + \alpha) + \left[1 + 2\alpha + 4\alpha^2\frac{x}{h}\left(1 - \frac{x}{h}\right)\right]\frac{t}{\delta}}, \quad (46)$$

where $\alpha = h/c$. The plots in Fig. 15a correspond to $\alpha = 3$, $\delta/h = \frac{1}{30}$, and the three selected values of the thickness ratio t/δ. The maximum torsion constant is attained when the spar is close to either left or right end of the profile. The minimum values $J_{\min} = 0.125 \times (4ch^2\delta)$ is in the middle of the span h ($x/h = 0.5$), regardless of the thickness ratio t/δ, because if $x = h/2$ there is no shear flow in the spar, and (46) reduces to a single-cell Bredt's formula $J = 2ch^2\delta/(1 + \alpha)$.

4.3. Two-cell elliptical profile

A two-cell thin-walled elliptical profile with the semi-axes a and b and the wall thickness δ is stiffened by a vertical spar of thickness t at the distance x from the center (Fig. 11b). Introducing the angle $\varphi = \sin^{-1}(x/a)$, there follows

$$A_1 = ab\left[\frac{\pi}{2} - \varphi - \frac{1}{2}\sin(2\varphi)\right], \quad A_2 = ab\left[\frac{\pi}{2} + \varphi + \frac{1}{2}\sin(2\varphi)\right],$$

$$I_{11} = 2\frac{a}{\delta}[E(\pi/2, e) - E(\varphi, e)] + 2\frac{b}{t}\cos\varphi,$$

$$I_{22} = 2\frac{a}{\delta}[E(\pi/2, e) + E(\varphi, e)] + 2\frac{b}{t}\cos\varphi,$$

$$I_{12} = -2\frac{b}{t}\cos\varphi, \quad e = (1 - b^2/a^2)^{1/2}. \quad (47)$$

The substitution of (47) into (32) yields an expression for the torsion constant, which can be evaluated numerically for any eccentricity of the ellipse and any thickness ratio t/δ. Fig. 15b shows the variation of the torsion constant with the spar distance x in the case $t/\delta = (0.5, 1, 2)$, the semi-axes ratio $a/b = 3$, and the thickness $\delta = a/15$. The maximum torsion constant in these three cases is $J_{\max} = (3.0204, 3.0494, 3.0762)a^2b\delta$, with the corresponding spars located at $x/a = (0.7933, 0.8021, 0.8107)$. When compared with the optimal location of the symmetrically positioned spars in a three-cell elliptical profile considered in Section 3.2, it is noted that the two spars there were closer to the center of the profile than is the single spar in the corresponding two-cell
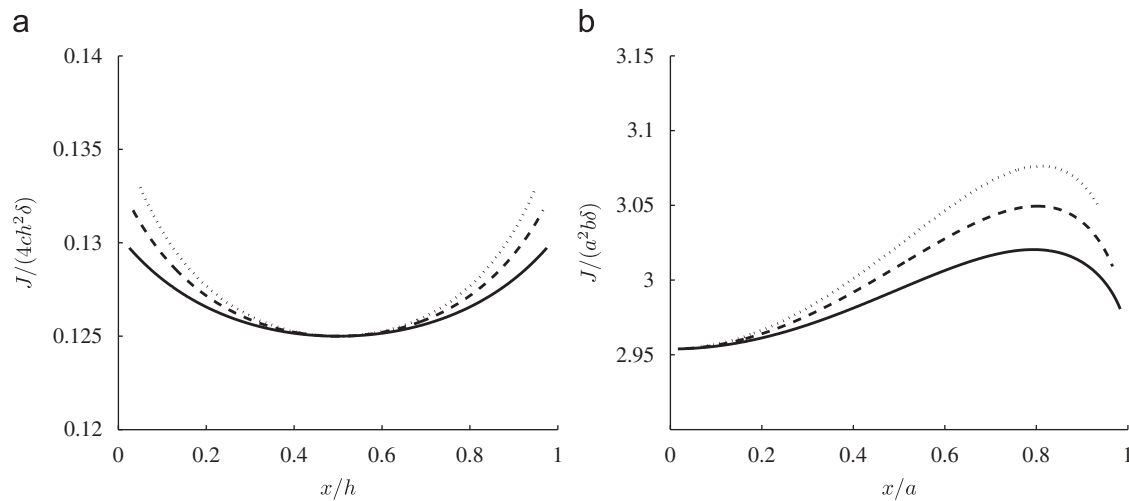
a

b

Fig. 15. (a) The variation of the torsion constant J with x/a for the rectangular profile from Fig. 14b with $c = h/3$ and $\delta = h/15$. The solid curve corresponds to the thickness ratio $t/\delta = 1/2$, the dashed curve is for $t/\delta = 1$, and the dotted curve is for $t/\delta = 2$. (b) The variation of the torsion constant of a two-cell elliptical profile from Fig. 11b, with $b = a/3$ and the same three wall-thickness ratios t/δ.

elliptical profile. Similar analysis can be done for triangular and semi-elliptical profiles of the type shown in Fig. 10, which are stiffened by one spar only. Details are omitted for brevity.

5. Conclusion

We have derived in this paper a closed-form expression for the torsion constant of thin-walled multicell profiles solely in terms of the geometrical properties of the profiles. Particularly appealing expressions are obtained in the case of structurally important two- and three-cell profiles. These expressions, previously not reported in the literature, greatly facilitate the determination of the optimal arrangement of internal spars which maximizes the corresponding torsion constant. Detailed analysis is performed for triangular, rectangular, elliptical and deltoidal thin-walled profiles. It is shown that the optimal location of spars for maximum torsion constant depends on the eccentricity of the ellipse, and the ratio of the internal and external wall thicknesses. For example, for a symmetric three-cell elliptical profile with the semi-axes ratio $a/b = 2$, and the uniform wall thickness $\delta = t = a/15$, the maximum torsion constant ($J_{\max} = 4.45a^2b\delta$) is attained when the two spars are located at the distance $0.786a$ from the center of the ellipse. If the elliptical profile is stiffened by only one spar, the maximum torsion constant ($J_{\max} = 4.245a^2b\delta$) is attained when the spar is located at the distance $0.812a$ from the center of the ellipse (in the case $a/b = 2$ and $\delta = t = a/15$). Similar conclusions apply to deltoidal and truncated deltoidal three-cell profiles. The conditions are also established for the inner wall to carry a prescribed portion of the shear flow, or no shear flow at all, with the application to two-cell trapezoidal and rectangular thin-walled profiles. For the trapezoidal profile with the steepness defined by $\alpha = 1$ and $\varphi = 15°$, the torsion constant is the greatest when the spar is located close to the larger base of the trapezoid. The minimum value of the torsion constant is attained at $x \approx 0.477h$, regardless of the thickness ratio t/δ, which corresponds to the shear-free spar location. For the triangular profile

with $\varphi = 15°$ and $\delta/h = \frac{1}{15}$, the maximum torsion constant is attained when the spar is located at the distance $x \approx 0.7h$ (mildly dependent on the thickness ratio t/δ). The minimum torsion constant corresponds to a shear-free spar, which is located at $x \approx 0.205h$, regardless of the thickness ratio t/δ. The obtained results are of importance on their own, and may also be useful for other studies of uniform and composite thin-walled beams and adaptive structures [10–12].

References

[1] Timoshenko SP. Strength of materials, part II: advanced theory and problems. 3rd ed. New Jersey: D. Van Nostrand; 1958.
[2] Peery DJ. Aircraft structures. New York: McGraw-Hill; 1950.
[3] Murray NW. Introduction to the theory of thin-walled structures. Oxford: Clarendon Press; 1984.
[4] Oden JT, Ripperger EA. Mechanics of elastic structures. New York: Hemisphere Publishing Corp.; 1981.
[5] Cook RD, Young WC. Advanced mechanics of materials. 2nd ed. Upper Saddle River, NJ: Prentice-Hall; 1999.
[6] Ugural AC, Fenster SK. Advanced strength and applied elasticity. 4th ed. Upper Saddle River, NJ: Prentice-Hall; 2003.
[7] Budynas RG. Advanced strength and applied stress analysis. 2nd ed. New York: McGraw-Hill; 1999.
[8] Boresi AP, Schmidt RJ, Sidebottom OM. Advanced mechanics of materials. 6th ed. New York: Wiley; 2003.
[9] Venkatraman B, Patel SA. Structural mechanics with introduction to elasticity and plasticity. New York: McGraw-Hill; 1970.
[10] Volovoi V, Hodges DH. Single- and multicelled composite thin-walled beams. AIAA Journal 2002;40(5):960–5.
[11] Loughlan J, Ahmed MN. Multi-cell carbon fibre composite box beams subjected to torsion with variable twist. Thin-Walled Structures 2008;46: 914–24.
[12] Cooper JE. Adaptive stiffness structures for air vehicle drag reduction. In: Multifunctional structures, meeting proceedings RTO-MP-AVT-141, France; 2006. p. 15-1–15-12.